

- 028715481

PUC - TN - 15/84

Nota Científica 15/84

DEUTERON- AND ALPHA PARTICLE- INDUCED
K-SHELL IONIZATION OF W AND Au ATOMS¹

F L Duarte Jr, E C Montenegro, J G de Faria
and G M Sigaud²

Departamento de Física, Pontifícia Universidade Católica,
Rio de Janeiro, CP 38071, RJ 22453, Brasil

ABSTRACT. Deuteron- and alpha particle- induced K-shell ionisation cross sections for W and Au were obtained from thick-target measurements for low impact velocities. They were compared to proton-induced cross sections in the same range of velocities. Equal-velocity cross sections ratios are a very stringent test to the corrections incorporated to the PWBA calculations. The c_2/v_p data presented in this paper sheds some light on the Coulomb-deflection corrections discussed in the literature. The consequences of the inelastic character of the ionisation process are thoroughly examined.

[Physics Abstracts: 34.50H]

¹Supported by Financiadora de Estudos e Projetos (FINEP).

²Permanent address: Instituto de Radioproteção e Dosimetria, CNEN, Rio de Janeiro, CP 37025, RJ 22700, Brasil.

1. INTRODUCTION

K-shell ionisation cross sections for W, Au and U by low-velocity protons measured in our laboratory were reported in a recently published paper (de Castro Laria et al 1984, hereafter referred as I). Good agreement was found between the experimental results and the PWBA predictions when binding, relativistic and Coulomb-deflection (monopole approximation) corrections are taken into consideration. The main experimental effort in I was to measure ionisation cross sections at proton energies where the projectile loses an important fraction (more than 7%) of its energy in the ionisation process. The good agreement between experimental and theoretical results is however partially lost when the inelastic aspect of the collision is added to the three aforementioned corrections. This fact casts some doubts about the suitability of correction procedures commonly used and points to the need of additional corrections or possible inconsistencies among them.

A deeper insight into this situation can be attained when equal velocity proton-, deuteron- and alpha particle-induced ionisation cross sections are compared (Basbas et al 1973, Lapicki et al 1980, Jesus and Lopez 1980, Rice et al 1981). From the experimental point of view the ratios of cross sections present uncertainties typically of about 2/3 of those obtained in individual cross section measurements due to the cancellation of some calibration quantities, when the same experimental set-up is used. On the other hand, the theoretical analysis of the results becomes easier since some

corrections almost completely cancel out in the equal-velocity cross section ratios.

Let the subscripts p , d and α refer to protons, neutrons and alpha particles, respectively. Protons and deuterons have the same nuclear charge and, at equal velocity, their energies are in the ratio $E_d/E_p = 2$. Binding effects must be essentially the same in both cases but different Coulomb-deflection and energy-loss effects are expected. On the other hand, deuterons and alpha particles having equal charge-to-mass ratio must exhibit the same Coulomb-deflection effect at the same velocity but different binding effects resulting from different projectile charges. By forming ratios of measured cross sections, σ_d/σ_p and $\sigma_\alpha/4\sigma_d$, the Coulomb-deflection and the increased binding effects can be isolated and better analysed, respectively. Moreover, the energy-loss effect, when present in the lowest proton energy cross sections, is much less pronounced for deuterons with the same velocity. Relativistic effects cancel out approximately in all ratios because the projectile velocities are the same.

In this paper we report W and Au K-shell ionisation cross sections for deuterons and alpha particles in the same range of velocities as for protons in I. Some σ_d/σ_p and $\sigma_\alpha/4\sigma_d$ ratios were measured at exactly $E_d = 2E_p$ and $E_\alpha = 2E_d$, respectively. The discussion of the results is primarily centered on the Coulomb factor and the effects of the energy loss of the projectile in the ionisation process.

2. EXPERIMENTAL TECHNIQUE AND RESULTS

The experimental set-up for the present measurements is fully described in 1. The W and Au targets were thick enough to stop the most energetic projectiles. The reduction of the rough data was performed as in 1. The function $y_x(E) = aE^2(1+bE^n)\exp(-cE^{-3/2})$ was adjusted to the experimental yield values by means of a weighted least squares fitting program (Bevington 1969). The resulting parameters are presented in table 1. The ionisation cross sections are given in table 2. Typical uncertainties in the absolute cross sections are from approximately 8% (Au) to 10% (W) for σ_c and 25% for σ_a .

In thick target measurements the cross section is proportional to the $dy_x(E)/dE$ derivative of the yield curve. A smoothing procedure by means of the fitting by a curve with n -adjustable parameters could give a unreliable result if the energy interval is too narrow and/or the number of available experimental points is too small. In the alpha particle measurements presented here the ratio $(E_a)_{\max}/(E_a)_{\min}$ is less than 2 and the number of measured values is of about $2n$. This is perhaps not enough to define accurately the local curvature of the yield curve. Then, despite the χ^2 of the fitting being vanishingly small, the errors associated to the adjustable parameters are too large and they are for the most part responsible for the large uncertainties in the reported values of σ_a . The information that could be drawn from such situation is probably too poor to allow definite conclusions.

It is worth mentioning that the nuclear Coulomb

excitation of the first excited states of the stable isotopes of K is an important source of uncertainty in the experimental determination of σ_{γ} . The contribution of γ_{IC} x-rays following the internal conversion is typically 2/3 of the observed γ_{IC} peaks. Good statistics is essential to ensure a safe subtraction of the x-rays resulting from primary nuclear processes. This implies the need of long runs (- 12h) and high currents (up to 500 nA) at the lowest incident energies.

3. DISCUSSION OF THE RESULTS

3.1. Absolute cross sections

In figure 1 the measured K-shell ionisation cross sections are compared with PWBA calculations (Rice et al 1977) including the increased binding effect (Basbas et al 1973, 1978), the correction due to the relativistic motion of the K-shell electron (Brandt and Lapicki 1979) and the deflection and deceleration of the projectile (Kochach 1976, Montenegro and de Pinho 1982). This calculated cross section is called σ_{PSSRC} . The same figure shows the theoretical results obtained by taking into account the energy loss of the projectile during the collision (σ_{EPSSRC}) as will be discussed in §3.3. The three usual corrections to PWBA deserve some remarks.

Discrepancies between approximate (Brandt and Lapicki 1979) and exact (Mukoyama and Sarkadi 1983) relativistic calculations increase as the projectile energy decreases. For protons on Au at 700 keV bombarding energy

the discrepancy amounts to about 25%, the relativistic effect being overestimated by the Brandt-Lapicki method.

Recently, Montenegro and Sigaud (1984) reexamined the problem of the adiabatic adjustment of the electronic wave function to the variable electric field of the target nucleus and projectile charges. As an alternative to the Basbas et al (1973) procedure they proposed the description of the binding effect by means of an average screening parameter \bar{Z} evaluated by using an energy-dependent united-atom nuclear charge. As the collision goes on, \bar{Z} follows a continuous function which reproduces the experimental values of the ionisation energies at the integer values of the nuclear charge variable. The values of \bar{Z} thus determined differ from the values of Z corrected by following the prescriptions of Basbas et al (1973) by 0.4 to 0.61 for alpha particles on W and Au, respectively. This effect is amplified by a factor of ten as the total cross section is calculated. So, if \bar{Z} is used instead of the PSS binding correction, a reduction of the calculated cross section for alpha particles on W (41) and Au (61) is obtained as compared with the PSS values, resulting in a better agreement with the alpha particle experimental data.

The adopted Coulomb factor was obtained assuming only monopole transitions. Gundersen et al (1982) have shown that the inclusion of the dipole contribution attenuates the Coulomb factor in the low-velocity region but that a strong cancellation of the dipole term by the recoil effect can occur in some cases. Rösler et al (1982) have demonstrated that with united-atom wave functions the recoil plus dipole

contribution to the T-matrix element is proportional to $(Z_t M_t - Z_i M_i)/(M_t + M_i)$ where the subscripts t and i stand for the target nucleus and the impinging particle, respectively. For heavy atoms like W and Au, $M_t/Z_t = 2.5$. For protons $M_i/Z_i = 1$ and for deuterons and alpha particles $M_i/Z_i = 2$. Then the cancellation is much more important for deuterons and alpha particles than for protons and the monopole approximation is more justified in the first cases than in the second one. Recently Graue et al (1984) have presented some numerical calculations that clearly demonstrate this peculiar feature of the dipole and recoil effects.

However, the monopole Coulomb factor gives also a satisfactory description of the proton experimental data reported in I. The consideration of the energy-loss effect results in a reduction of the low energy cross section that probably compensates the increase of the cross section due to the dipole plus recoil term contribution. The character of this discussion is of course merely qualitative.

3.2. Cross section ratios

The σ_d/σ_p ratio is a very stringent test for the Coulomb factor since it is almost independent of both binding and relativistic effects. Figures 2 and 3 show that the adopted Coulomb correction gives much better agreement with the experimental points than that proposed by Basbas et al (1973). The need of a Coulomb factor steeper than this last one has already been discussed by Paul (1982).

For velocities corresponding to energies greater than -1 MeV/u , the monopole approximation gives a satisfactory description of the situation, as expected from the preceding discussion, but as the impact velocities become very low the experimental points are increasingly above the theoretical results. In the case of Au the theoretical results are improved when the inelastic character of the collision is considered but the situation is inverted in the case of W where the correction is obviously excessive.

The inclusion of the dipole plus recoil effects would result in a theoretical curve somewhere between the solid and the broken lines of figures 2 and 3. As will be discussed later, residual effects of the incomplete compensation of the energy loss correction, on the one hand, and the dipole correction, on the other hand, not clearly observed in the total cross section versus energy curves are magnified in the σ_d/c_p ratios because of the cancellation of other effects.

The $c_a/4c_d$ ratio could give some information about the binding correction. However, as mentioned before, the large uncertainties in the alpha particle cross sections render hazardous any quantitative conclusion. The $c_a/4c_d$ measured ratios are systematically too small as compared with the theoretical predictions even when the procedure proposed by Montenegro and Sigaud (1994) for calculating the binding effect is used.

3.3. The energy loss effect

The correct limits of integration over the momentum and energy transfers are not considered in the published PWBA tables except in that of Benka and Kropf (1978). In the transition of an independent electron from an initial bound state with energy E_0 to a final state with energy E_n the energy transferred to the electron by the projectile is $\hbar\omega = E_n - E_0$. If this energy is small as compared with the incident energy it is usual to consider the minimum momentum transfer $q_{\min} = \omega/v$ and the maximum momentum transfer $q_{\max} = \dots$, where v is the incident velocity. Within this approximation, very simple scaling laws for the total cross section are obtained since the velocity and the charge are the only relevant parameters associated to the projectile. When the correct limits of integration are taken into account a dependence on the reduced mass of the colliding system appears.

In order to preserve the parametrization and the same functional dependence of the total cross section on the scaled incident energy n , Montenegro et al (1981) proposed the simulation of the effect of considering the correct limits of integration through the use of an effective velocity defined in such a way that $q_{\min} = \omega/v_{\text{eff}}$. Here $v_{\text{eff}} = v\sqrt{1 + (1-\epsilon)^{1/2}}/2$ with $\epsilon = 9m_0^2/BM$ where, as before, ϵ is the scaled binding energy and m_0/M is the ratio of the electron mass to the reduced mass of the system.

Since the integration over the momentum transfer is

now from $q_{\min} = c/v_{\text{eff}}$ up to $q_{\max} = \infty$ the incorrect PWBA tables for the function $F(n/c^2, 0)$ can be used with n replaced by v_{eff} where, obviously, $v_{\text{eff}} = n(v_{\text{eff}}/v)^2$. As it was emphasized in the paper of Montenegro et al (1981), when the total cross section is calculated the function F must be multiplied by v_{eff}/v in order to restore the flux conservation in the process of scattering.

It is well known the equivalence between the total ionisation cross sections obtained in the PWBA (with the integration over q from $q_{\min} = c/v$ to infinity) and in the semiclassical approximation (with straight-line trajectory, SL-SCA) (Bethe and Jackiw 1968). As the lower limit q_{\min} of PWBA is modified to c/v_{eff} the equivalence still holds if the asymptotic velocity in the SL-SCA is made equal to v_{eff} .

Let $v(n)$ and $v'(n')$ represent the asymptotic incident and emergent velocities (reduced energies), respectively. Then $n' = n - (n/M)\bar{W}$ where \bar{W} is the average energy transfer in the adiabatic limit, $\bar{W} = 96/8$. From the definitions of v_{eff} and β , it follows that $n' = n(1 - \beta)$, then $\beta = 1 - (v'/v)^2$ and $v_{\text{eff}} = (v+v')/2$. Thus v_{eff} is the so-called symmetrized velocity. The proposed simulation of the correct limits of integration automatically introduces the idea of a symmetrized velocity.

To be more specific, one must compare the PWBA cross section for the transition $0 \rightarrow n$

$$\sigma_{0 \rightarrow n}^{\text{PWBA}} = 8\pi \left(\frac{Z_1 e^2}{\hbar v} \right)^2 \int_{c/v_{\text{eff}}}^{\infty} \frac{dq}{q^3} \left| \int v_n^*(\mathbf{r}) \exp(i\mathbf{q} \cdot \mathbf{r}) \psi_0(\mathbf{r}) d^3r \right|^2 \quad (1)$$

with the equivalent EL-SCA cross section

$$\sigma_{0-n}^{SCA} = \left(\frac{v_{eff}}{v} \right)^2 \left(\frac{4\pi^2 Z_1 e^2}{\hbar} \right)^2 \int_{-b}^b dp |p| \left| \int_{-\infty}^{\infty} dt e^{iut} \left| \frac{v_{in}^*(\vec{r}) v_o(\vec{r})}{|\vec{r}-\vec{R}(t)|} \right| d^3r \right|^2 \quad (2)$$

In the straight-line approximation the projectile moves along the trajectory $\vec{R}(t) = \vec{p} + \vec{v}_{eff}t$, where p is the impact parameter. In equation (1) c/v_{eff} replaces the commonly used value c/v . There is equivalence between the two equations because at the same time that the matrix element in equation (2) was modified through a redefinition of $\vec{R}(t)$ in terms of v_{eff} , a factor $(v_{eff}/v)^2$ was introduced in order to restore the correct incident flux. The matrix element is then symmetrized, but the cross section σ_{0-n} is not. This symmetrization procedure is exactly alike that proposed by Alder et al (1956) in the nuclear Coulomb excitation problem.

Now, when $R(t)$ describes hyperbolic paths it seems natural to extend the concept of effective or symmetrized velocity to these trajectories. Then, after expressing the Coulomb factor in terms of v , this parameter must be everywhere replaced by v_{eff} .

The σ_{EP5SRQ} results presented in figures 1 to 3 were calculated with v replaced by v_{eff} everywhere with the caution of maintaining the correct incident flux. This procedure gives, within 3%, the same numerical values as those obtained with the Brandt and Lapicki (1981) prescriptions to take into account the energy loss. The present procedure presents the double advantage of being much more simple and treating the

correction for the exact limits of integration and the symmetrization in a consistent way.

In figure 4 the ratio $\sigma_{EPSSRC}/\sigma_{PSSRC}$ is plotted against $\log \xi$, where ξ is the parameter $2v^{1/2}/v$. This was done to make easier the comparison with the figure 3 of the paper of Graue et al (1984). As far as the Z_1 , Z_2 , and Z_t dependences are concerned, it is evident that the energy loss and the dipole effects show some sort of complementary behaviour. The consequence is a partial compensation of both effects over broad intervals of energy for a given projectile-target pair. For the projectile-target combinations studied in the present work the compensation seems to be rather complete for deuterons and alpha particles on W and Au. The residual effect of both corrections is at most of the order of a typical error bar in the experimental cross sections. For protons, where both effects are much more important, for $\log \xi \leq -0.75$ the compensation is incomplete and the energy loss effect dominates. This prediction conflicts with the experimental results presented in I for $E_p \leq 1.25$ MeV. When the dipole to monopole contribution ratios calculated by Graue et al (1984) for $Z_t = 81$ are used for the $Z_t = 79$ data, the σ_{EPSSRC} points in figure 3 are reduced by 17% at 0.71 MeV/u, 13% at 0.82 MeV/u, 9% at 1 MeV/u and 5% at 1.25 MeV/u. In figure 5 the experimental and theoretical values for the σ_d/σ_p cross section ratios are compared. In its upper part the theoretical results are PSSRC values; in its lower part they are EPSSRC values including, for both W and Au, the same dipole contribution calculated for Pb by Graue et al (1984). Although this correction has been introduced in an ad hoc manner, it is expected to be quite satisfactory and it greatly improves the agreement between theory and experiment.

4. CONCLUSIONS

The determination of ionisation cross sections at the extreme low velocity region is a very difficult task from both experimental and theoretical points of view. Uncertainties less than 10% are not easy to be reached especially when thick targets are employed. The cross sections are so small in this region and depend so strongly on the energy that a compromise between a reasonable counting rate and the troubles with the energy degradation of the projectile inside the target is a permanent challenge. On the other hand, in the theoretical results the interdependence among the different corrections incorporated to the basic PWBA calculations renders very dangerous the uncritical extrapolation of procedures and prescriptions that reproduce well the experimental data in some regions of velocities and projectile-target combinations to other ones. Particularly in the extreme adiabatic region the total cross section is highly dependent on subtle details in the treatment of these corrections since the strong dependence on η and ζ magnifies very small changes of these parameters. A unsuspected correlation between energy-loss and dipole effects was pointed out by the data discussed in this paper; it is not clear whether it is accidental or it lies on more fundamental aspects of the interaction and/or of the formalism. It is important to pursue some kind of parametrization in terms of effective variables (velocities, energies, charges and masses) but a case by case numerical calculation is essential when an exact description of

each projectile-target pair ionisation cross section is
desired.

REFERENCES

- Alber K, Rohr A, Huot T, Mottelson E and Winther 1966 *Rev. Mod. Phys.* 28 432
- Asker C, Brandt W and Laubert F 1973 *Phys. Rev.* A7 983
- _____ 1978 *Phys. Rev.* A17 1655
- Benka C and Tropp A 1978 *At. Data Nucl. Data Tables* 22 218
- Bethe H A and Jackiw 1968 *Intermediate Quantum Mechanics*, 2d ed. (New York: Benjamin)
- Bevington F K 1969 *Data Reduction and Error Analysis for the Physical Sciences* (New York: McGraw-Hill)
- Brandt W and Lapicki G 1979 *Phys. Rev.* A20 465
- _____ 1981 *Phys. Rev.* A23 1717
- de Castro Faria N V, Freire Jr F L, Montenegro E C, de Pinho A G and da Silveira E F 1984 *J. Phys. B: At. Mol. Phys.* 17 (in press)
- Graue A, Hansteen J M and Kocbach L 1984 Scientific Report No. 144, University of Bergen, Norway
- Gundersen K, Hansteen J M and Kocbach L 1982 *Nucl. Instrum. Meth.* 192 63
- Jesus A P and Lopes J S 1980 *Proc. Int. Conf. on X-ray processes and inner shell ionisation* ed E J Fabian, H Edlén, J. J. Haughey and L M Watson (New York: Plenum) p 21
- Kocbach L 1976 *Phys. Norv.* 8 187
- Lapicki G, Laubert F and Brandt W 1980 *Phys. Rev.* A22 1889

CAPTIONS TO FIGURES

- Figure 1. Deuteron (solid circles) and alpha particle (open circles) induced K-shell ionisation cross sections versus energy. The solid curve is σ_{PSSRC} and the dashed curve is σ_{EPSSRC} .
- Figure 2. Ratio of measured cross sections for deuterons and protons of the same velocity impinging on a thick target of tungsten. The curves are: — PSSRC predictions with the Montenegro and de Pinho (1982) Coulomb factor; ---- EPSSRC predictions with the same Coulomb factor as before and the energy loss correction described in the present paper; -.-. EPSSRC predictions with the Coulomb factor of Basbas et al (1973).
- Figure 3. The same as figure 2 for a target of gold.
- Figure 4. The ratio $\sigma_{EPSSRC}/\sigma_{PSSRC}$ versus $\log \xi$ for different targets (Ni, Ag, Au) and projectiles: — protons; ---- deuterons; -.-. alpha particles.
- Figure 5. Ratios of experimental to theoretical deuteron- and proton- induced ionisation cross section ratios. Solid circles are the W data and open circles are the Au data. In the upper part of the figure the theoretical results are PSSRC values and in the lower part they are EPSSRC values including an estimate of the dipole contribution.

TABLE 3

	a	b	c	t
d on W	10.2 (1.7)	8.26×10^{-2} (2.0)	2.45 (1.0)	5.80 (2.5)
d on Au	8.74 (1.3)	1.35×10^{-5} (2.7)	3.36 (0.5)	7.09 (4.3)
H α^+ on W	3.20 (9.9)	6.37×10^{-6} (57.3)	4.12 (10.5)	15.9 (6.6)
H α^+ on Au	1.41 (20.6)	2.41×10^{-8} (46.0)	7.65 (4.3)	20.4 (11.8)

Montenegro E C, de Lima A C and Faria J Jr. (1981) J. Phys.
B: At. Mol. Phys. 14 1591

Montenegro E C and de Lima A C 1982 J. Phys. B: At. Mol. Phys.
15 1521

Montenegro E C and Figueira G M 1984 J. Phys. B: At. Mol. Phys.
(submitted for publication)

Nakayama T and Ferrelis I 1963 Phys. Rev. A26 1303

Paul H 1962 Nucl. Instrum. Meth. 192 11

Rice K E, McDaniel F D, Hueston G and Duggan J L 1961 Phys. Rev.
A24 756

Rösel F, Trautmann D and Baur G 1962 Nucl. Instrum. Meth. 162 43

CAPTIONS TO TABLES

Table 1. The adjustable parameters in the fitting of the yield vs energy curve. Numbers in parentheses indicate the standard deviation in percent.

Table 2. Measured F-shell ionization cross sections in b. Numbers in parentheses indicate powers of 10. Experimental uncertainties are discussed in the text.

TABLE 2

K ($\epsilon_p = 0.927$, $r_p/r_o = 0.275$)				Ku ($\epsilon_p = 0.964$, $r_p/r_o = 0.275$)			
E_D (M-V)	c_j^1 (lb)	r_o (M-V)	c_j^2 (lb)	E_D (M-V)	c_j^K (lb)	L_o (M-V)	c_j^K (lb)
1.36	1.12(-4)	1.20	5.56(-5)	1.42	6.85(-5)	2.60	7.36(-5)
1.44	1.97(-4)	2.40	1.68(-4)	1.52	1.24(-4)	2.64	1.33(-4)
1.60	3.27(-4)	2.60	2.05(-4)	1.64	1.84(-4)	3.04	2.02(-4)
1.70	4.78(-4)	2.86	4.44(-4)	1.80	2.83(-4)	3.28	3.20(-4)
1.80	5.45(-4)	3.20	7.11(-4)	1.90	3.56(-4)	3.60	5.83(-4)
1.90	6.80(-4)	3.40	9.17(-4)	2.00	4.38(-4)	3.80	7.91(-4)
2.00	8.29(-4)	3.60	1.12(-3)	2.25	6.95(-4)	4.00	1.14(-3)
2.25	1.28(-3)	3.80	1.42(-3)	2.50	1.01(-3)		
2.50	1.87(-3)	4.00	1.74(-3)	2.75	1.44(-3)		
2.75	2.55(-3)			3.00	1.96(-3)		
3.00	3.48(-3)			3.25	2.67(-3)		
3.25	4.54(-3)			3.50	3.53(-3)		
3.50	5.79(-3)			3.75	4.52(-3)		
3.75	7.27(-3)			4.00	5.85(-3)		
4.00	9.11(-3)						

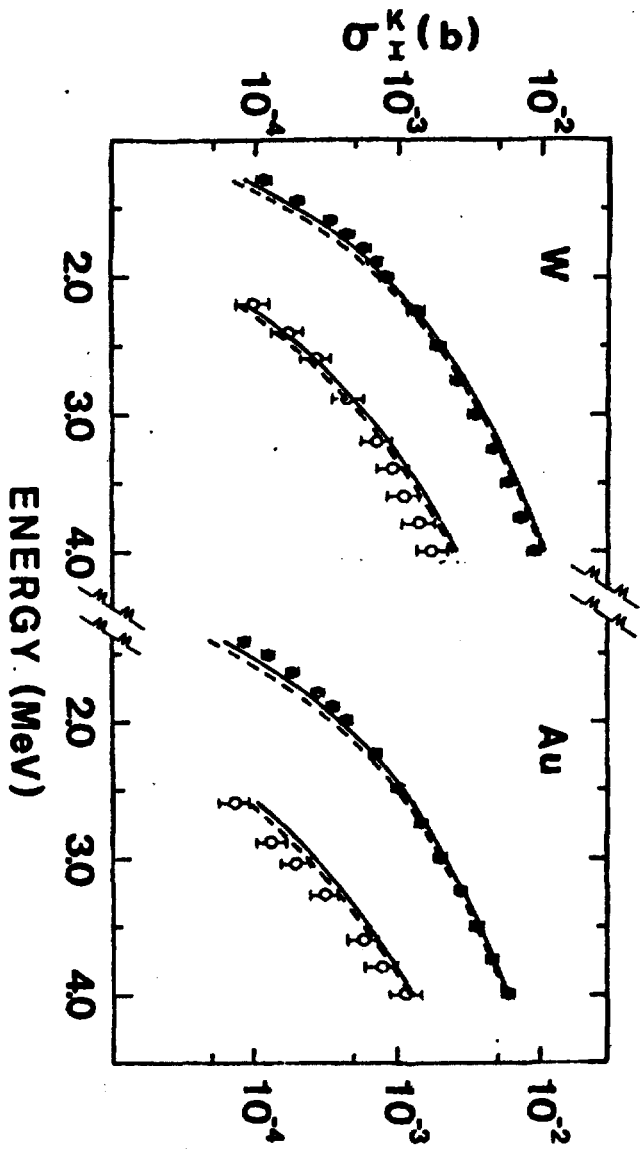


Figure 1

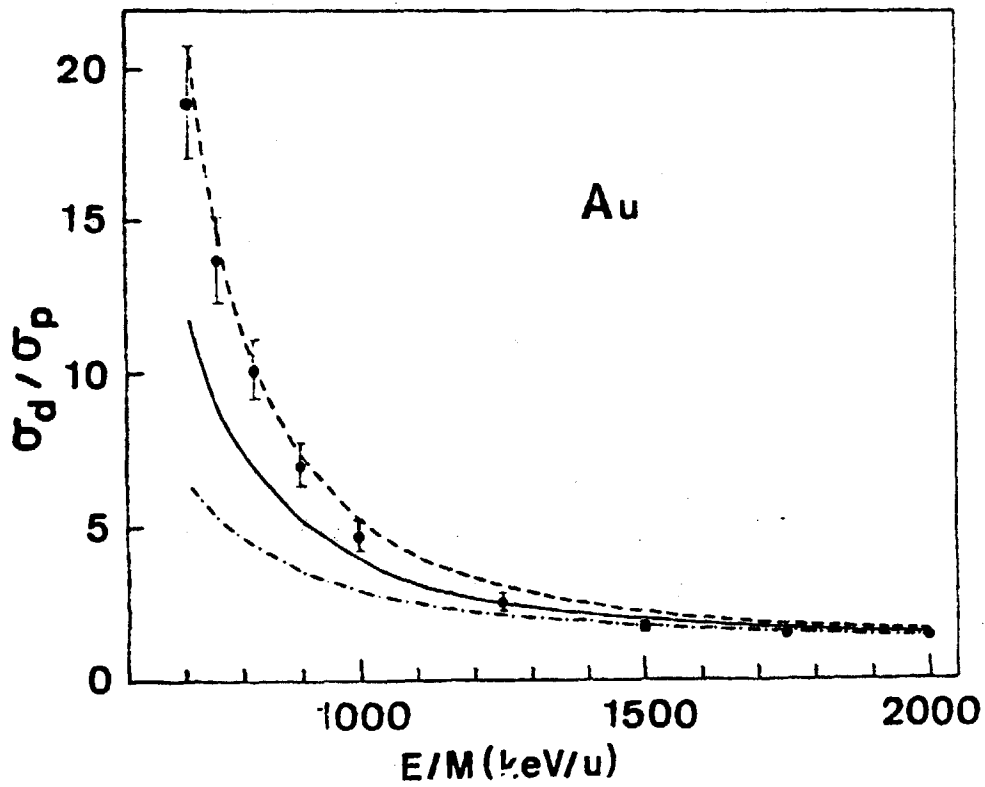


Figure 3

Fig 3

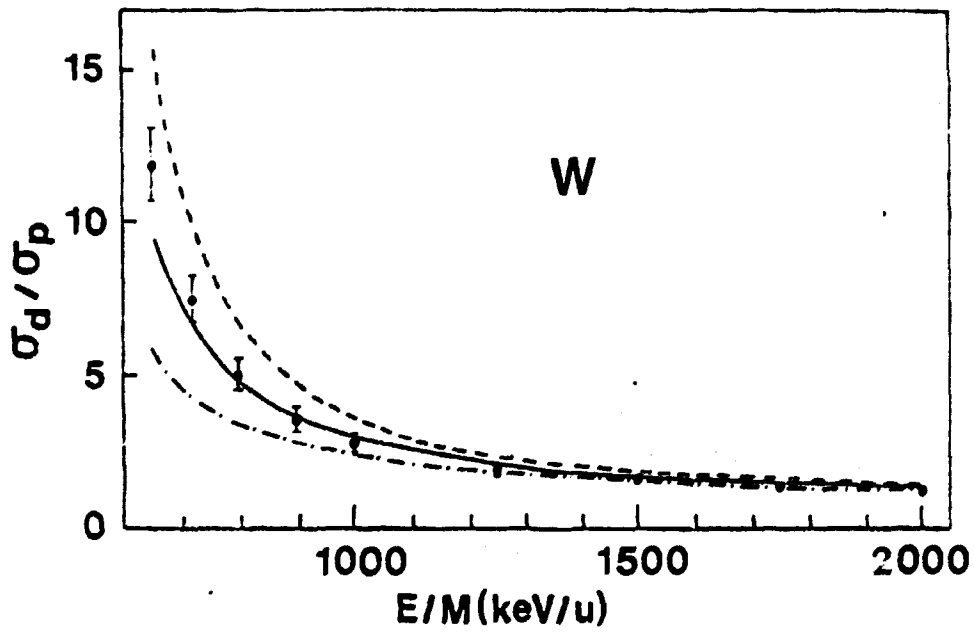


Figure 2

Fig 2

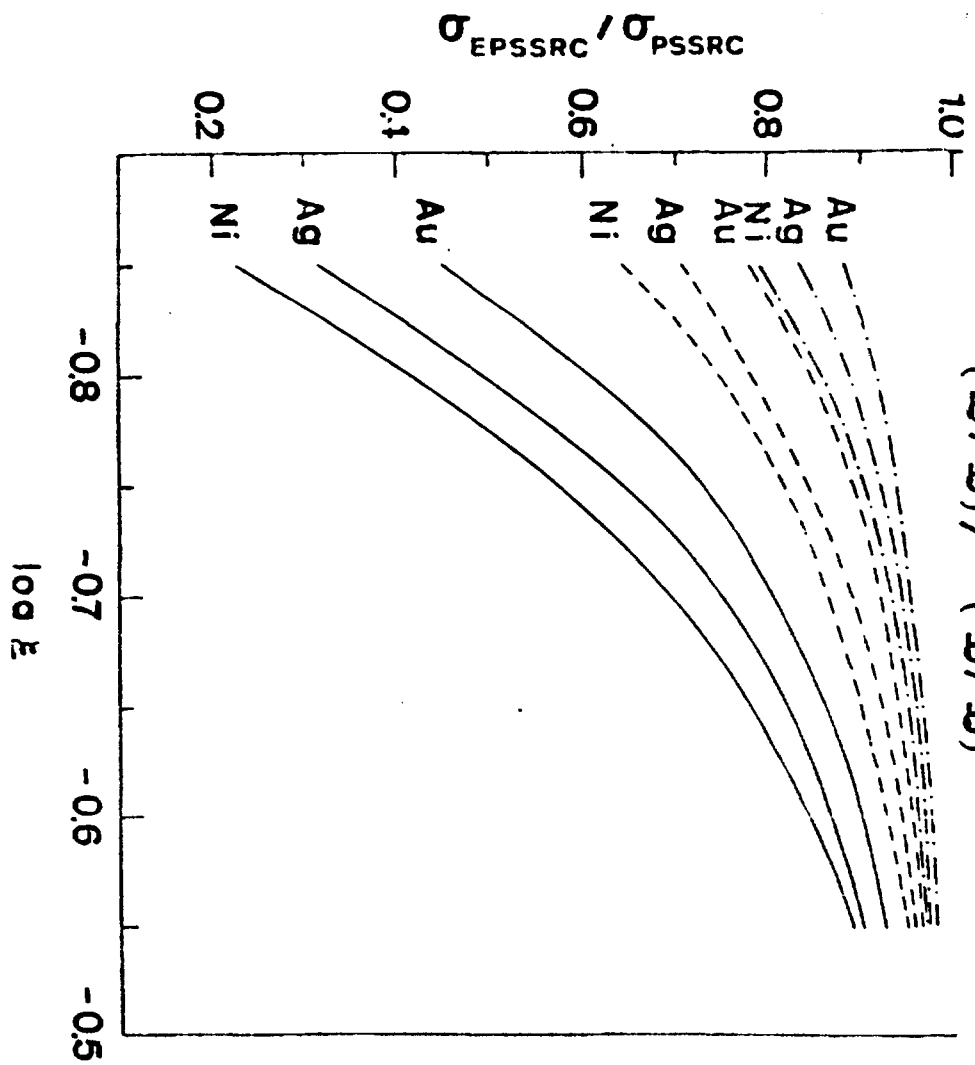


Figure 4

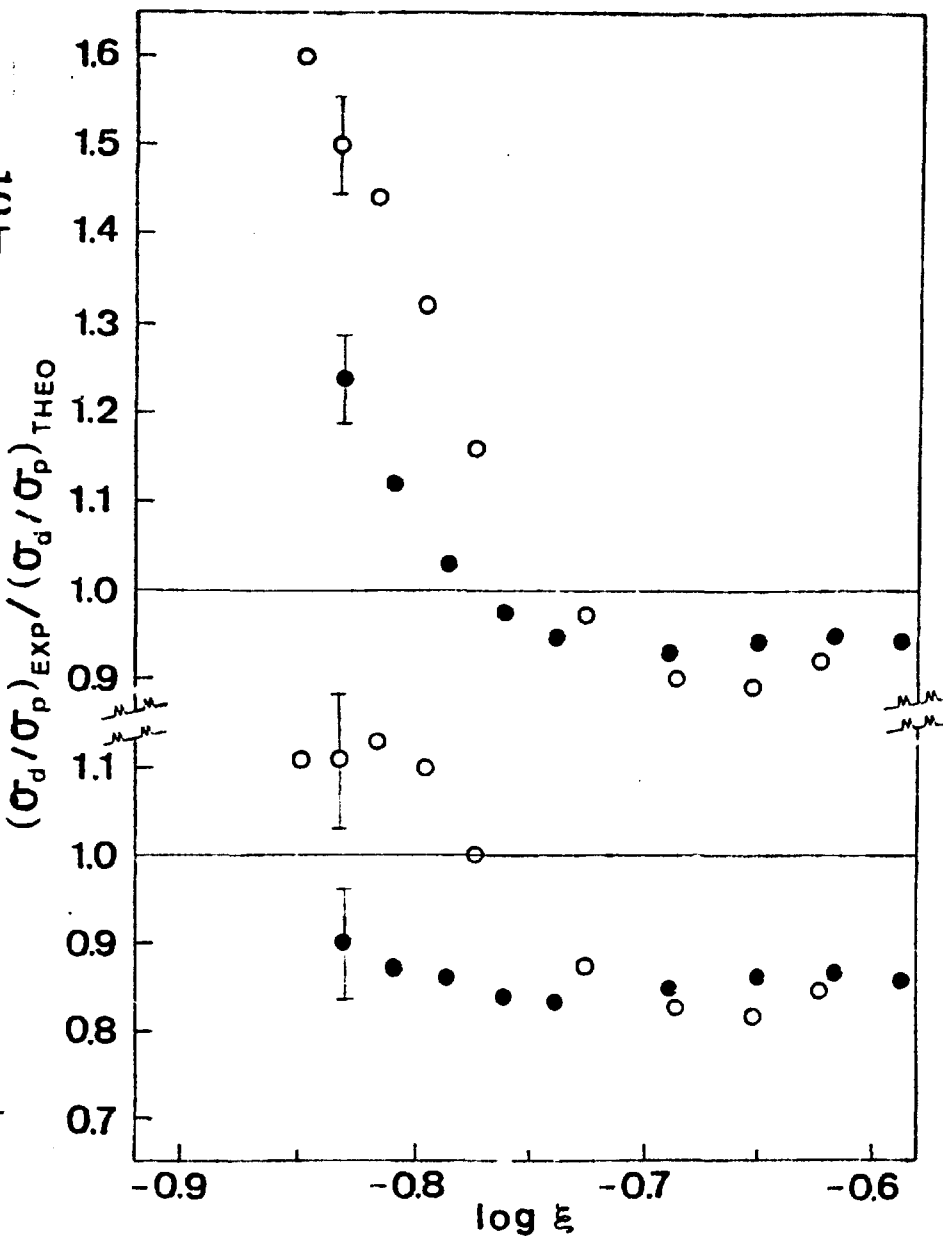


Figure 5

6.1.4